Surface & Coatings Technology 284 (2015) 400–403

Contents lists available at ScienceDirect

Surface & Coatings Technology

journal homepage: www.elsevier.com/locate/surfcoat

Thin films growth by PIIID technique from hexamethyldisilazane/argon mixture

F.V.P. Kodaira *, R.P. Mota, P.W.P. Moreira Jr

São Paulo State University — UNESP, Guaratinguetá, SP 12516-410, Brazil

ARTICLE INFO

Article history:
Received 25 March 2015
Revised 2 September 2015
Accepted in revised form 7 September 2015
Available online 22 October 2015

Keywords:
PIIID
HMDSN
Plasma polymer
Physical properties
Chemical structure

ABSTRACT

Plasma polymer thin films are pinhole-free and have also a high cross-linked structure. These kinds of films are insoluble in mild acids and bases and present good adhesion on different materials. These features make the films relevant for industrial applications and are used in different fields such as electronics, mechanics, biomedics, electrics, protective coatings and others. The plasma polymer hexamethyldisilazane/argon films (ppHMDSN/Ar) were deposited on substrates which were placed between two stainless steel parallel plate electrodes fed by a radio-frequency source operated at 13.56 MHz and 50 W at a total pressure (HMDSN and argon) of 80 mTorr. The negative bias of 10 kV and 10 Hz pulse were used for ion implantation. The structural characterization of the films was done by FTIR spectroscopy. The contact angle for water was of approximately 98° and the surface energy of 30 mJ/m^2 which represents a hydrophobic surface, measured by goniometric method. The refractive index of these materials presents values from 1.56 to 1.64 measured by ultraviolet–visible technique. The thickness of the samples was measured by profilometry and showed values from 96 to 210 nm for different deposition conditions resulting in deposition rates from 4.8 to 10.5 nm/min. Hardness values ranging from 0.9 to 2.6 GPa were found for the films measured by nanoindentation technique.

1. Introduction

Plasma immersion ion implantation and deposition (PIIID) is an important process for the production of novel materials [1–5]. Plasma polymers which have specific mechanical, electrical, optical and wettable properties and which also show good adhesion to the substrate may be produced. Although applications of plasma polymerization are of growing technological importance, the processes that take place in the plasma are poorly understood. PIIID is a highly efficient technique for surface modification of metals, semiconductors, ceramics and polymeric materials and on this account, it has been employed in different areas, such as aeronautics, optics, biomedics, coatings and electronics [6–16]. In this implantation and deposition process, the substrates (or samples) are immersed in the plasma and are polarized with high voltage pulses. In this specific process of ion implantation and plasma polymerization, ions are accelerated toward the deposited polymer and are implanted into its structures. This bombardment promotes bond breakage and recombination process in the chemical structure of the material and, consequently, it causes modifications in its chemical, optical, mechanical, biological and tribological properties. Nevertheless, the degree of these modifications strongly depends on plasma parameters (power, frequency, pressure, and gas species), pulse characteristics (amplitude, repetition rate and work time). In this work, hexamethyldisilazane (HMDSN) was used as monomer and argon as a source of ions. The argon does not directly react with the growing polymer but it increases the plasma fragmentation of HMDSN, changing the nature of film precursors as well as the chemical composition of the deposits. Argon ions, on the other hand, can be implanted in the growing film changing its structure and/or its chemical composition [9]. HMDSN films are interesting to many applications, as optical, protective and biocompatible coatings. Refractive index and hardness were correlated to the molecular chemical modifications of the samples induced by PIIID technique and sample wettability was also investigated.

2. Experimental setup and measurements

The PIIID occurs inside a cylindrical stainless steel reactor whose diameter is 21.5 cm and height is 24.5 cm, with pipes for vacuum pumping, controlled gas admission, and optical observation. Inside the reactor there are two parallel stainless steel disk shaped plain electrodes with a gap of 3 cm between them. The upper electrode is biased by a 50 W and 13.56 MHz radio-frequency power source for the deposition, while the lower one is fed by a 10 Hz and −10 kV high voltage power source for the ion implantation, both processes occurs simultaneously. Fig. 1 shows a scheme of the system. The substrates are placed on this lower electrode, two different substrates were used for the measurements, the FTIR analysis was performed on films deposited on aluminum foil substrates, the contact angle, hardness and thickness on

* Corresponding author at: UNESP, Av. Dr Ariberto Pereira da Cunha, 333, Pedregulho, 12516-410 Guaratinguetá, SP, Brazil
E-mail address: kodaira.felipe@gmail.com (F.V.P. Kodaira).

http://dx.doi.org/10.1016/j.surfcoat.2015.09.063
0257-8972/

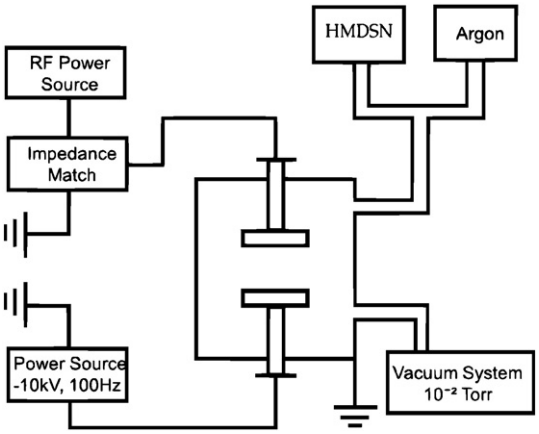

Fig. 1. Scheme of the system used for the PIIID process.

microscope glass slide substrates and the refractive index on quartz substrates.

When the pumps are switched on, a pressure of 10^{-5} Torr is reached, in order to clean the system. After that, the turbomolecular pump is switched off and the mechanical pump keeps the system at 10^{-3} Torr. HMDSN enters the reactor by a precise needle valve until it reaches the required pressure, then argon is added until the pressure rises to 80 mTorr. The aim is to vary the proportion of HMDSN and argon inside the chamber in steps of 10 mTorr so that the sum of both is equal to 80 mTorr in each deposition. The RF power was 50 W, while the high voltage was maintained in negative 10 kV and 100 Hz frequencies. The process time was 20 min.

The FTIR spectra for the films were collected by a FTIR spectrometer Perkin Elmer Spectrum 100 which operated in the spectral range from 4000 to 400 cm^{-1}. The contact angle and surface energy measurements were performed by using a goniometer Ramè Hart — 300F1 controlled by a computer. The refractive index of the samples was measured by a Perkin Elmer Lambda 25 UV/VIS spectrometer. Hardness was determined by nanoindentation experiment performed in a Hysitron Triboindenter system in which a controlled load, ranging from 1 to 10 μN could be applied by a Berkovich diamond indenter. Those hardness measurements were carried out in eight different positions of each film and ten different maximum loads were used (20–1000 μN) in each of them. This resulted in 80 indentations per sample. The thickness of the samples was measured by profilometry technique by using an Alpha Step Tencor 100 profilometer.

2.1. Infrared analysis

Fig. 2 shows the transmittance spectra of PIIID films from the HMDSN/Ar mixture. The analysis has been carried out in the range of 4000–650 cm^{-1}. The curves have been offset vertically for clarity. The transmittance spectra show the characteristic peaks [3,17–18] summarized in Table 1. The intensity of the absorption band associated to the N–H bond is weaker at HMDSN(20)/Argon(60) mTorr partial pressure. Inelastic collisions with energetic electrons or other reactive species causes a large breaking of N–H bonds in the plasma phase [17]. The peak associated with CH_2 groups, which is not present in the monomer, rose due to the extraction of hydrogen by breaking C–H bonds in methyl groups. Increase of the argon proportion inside the chamber promoted a higher fragmentation of HMDSN, as the peaks associated to C–H and Si–CH_3 bonds decrease. The high fragmentation of the organic molecules produces smaller molecules, many of them are volatile and are pumped out by the vacuum system, and so, the film grows more inorganic. Peaks related to oxidized molecules are also present in the spectra, since they are not present in the monomer The origin of this contamination from oxygen may originate from the desorption of the residual oxygen from the chamber wall during the process or by the contact with the atmospheric oxygen and moisture when the film is exposed to the environment.

2.2. Thickness and deposition rate

The deposition rate of the films as a function of HMDSN/Ar ratio is shown in Fig. 3. Two processes are responsible for reducing the deposition rate: ablation that causes loss of atomic and molecular species and cross-linking of chains which enhances the film density. Both processes can occur simultaneously but the predominance of each one depends on partial pressure. When an ion impinges on the film, its energy is transferred to the structure via atom collision and this energy transfer continues to neighboring atoms until one of them is emitted from the surface to the plasma, since the argon is relatively heavy the sputtering process is more effective for higher rates of it and it is expected that the argon ion implantation increases the sputtering in the film for the applied electric field accelerates the ions toward the samples, reducing its thickness. Another reason for the reduction in film thickness during ion implantation is the film structure densification through cross-linking and unsaturation process. After energy transfer, several physical and chemical processes take place in the film structure, such as electronic excitation, ionization and hydrogen emission, among others. Such events result in the free radical generation or dangling bonds, which lead to the formation of unsaturated bonds, as well as the cross-linking of neighboring chains. Both sputtering and cross-linking processes occur simultaneously and vary when the partial pressure changes in the plasma. But one of them may dominate depending on the argon pressure. When argon quantity increases the probability of deposition rate decreasing is higher, also the lower the concentration of HMDSN on the mixture, the lower the amount of the film precursor, causing the film to grow slower [19]. This observation is in agreement with the results obtained in other studies in which plasma polymerized acetylene and HMDSN films treated with nitrogen by using plasma immersion ion implantation and plasma immersion ion implantation and deposition. [3,17–20].

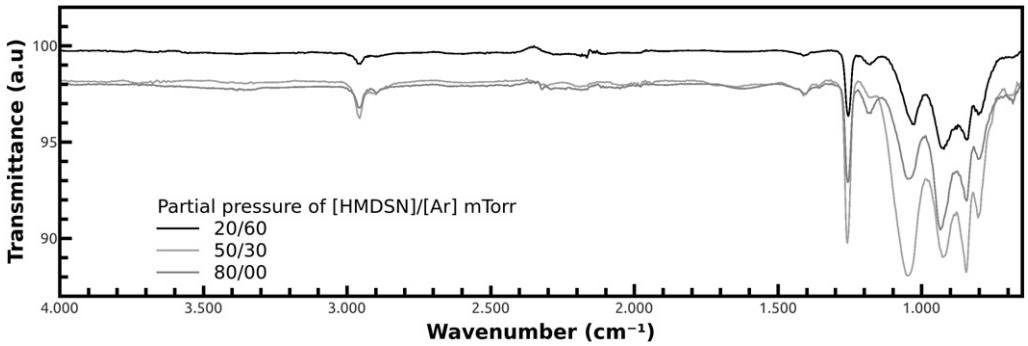

Fig. 2. Infrared spectra of HMDSN(mTorr)/Ar(mTorr) PIIID films deposited at 50 W radio-frequency power.

Table 1
FTIR band assignment of HMDSN/Ar PIIID films.

Peak position (cm^{-1})	Band assignment
2960	ν_a (C–H) in CH_3
2900	ν_s (C–H) in CH_x
2130	ν Si–H_x in (Si–H)
1410	δ_a (CH3) in Si–(CH3)x
1260	δ_s (CH3) in Si–(CH3)x
1180	δ (N–H)
1100–1025	δ_a (Si–O) in Si–O–Si
1025	w (CH_2) in Si–CH_2–Si
930	δ (Si–H)
850	ρ (CH3) in Si–(CH3)3
800	ν (Si–C) in Si–(CH3)2
680	w (Si–H)

ν: stretching; δ: bending; ρ:rocking; w: wagging; a: asymmetric; s: symmetric.

2.3. Optical properties — refractive index

Refractive index values n were determined for films which were deposited from HMDSN/Ar discharges at several partial pressures. Ultraviolet–visible spectra provided the basis for the calculations, which were made according to the procedure used by Cisneros et al. [20–22]. The value of n for photon energy of 1 eV is shown in Fig. 3. The refractive index decreases from 1.64 to 1.56 as the argon proportion in HMDSN/Ar ratio increases. This slight tendency in the behavior of the refractive index was also observed in films obtained by PIIID of HMDSN/nitrogen [3]. The alterations in the optical properties of the films can be attributed to the random structure of the chains in a plasma polymer, which makes theoretical interpretation of the experimental results rather difficult. However, it is possible to suppose that some trends in the physical behavior of a "conventional" polymer must be followed by a HMDSN/Ar PIIID polymer film. For example, the density of π bonds is influenced by the degree of hydrogenation, which, as discussed in FTIR analysis, depends, on the other hand, on the different concentrations of HMDSN and argon in the PIIID process. The detachment of hydrogen from the films also affects bond lengths, and changes the band gap and the refractive index. These hypotheses emphasize the current lack of understanding of the relationship between the optical and structural properties of PIIID polymer films.

2.4. Hardness

The hardness of the films produced at different partial pressures of HMDSN/Ar plasmas are shown in Fig. 4. These measurements were obtained at a depth of 30 nm which represents from 15 to 30% of the sample thickness. Therefore, the glass substrate is not expected to influence the results. Film hardness increases monotonically as argon increases in HMDSN/Ar ratio in the plasma immersion ion implantation and deposition process. The hardness of HMDSN plasma polymer is near 0.7 GPa and is in agreement with other plasma polymer films as acetylene, benzene, hexamethyldisiloxane [23,24]. This level of hardness is slightly higher than the hardness of 0.5 GPa found in "conventional" polymers [23]. It can be seen that the HMDSN/Ar film hardness rose from 0.7 to 2.6 GPa as the argon increased in HMDSN/Ar ratio. The hardness increased almost three times more than the initial value. The presence of argon in the discharge may have resulted in a more effective bombardment process than that produced in pure hexamethyldisilazane plasma. The introduction of a noble gas alters the process kinetics and so the properties of the resulting films. It confirms the unsaturated and cross-linking process enhancement which was suggested before. This way, it is necessary to emphasize that ion implantation usually promotes modifications of the film structure. The effect of ion implantation during deposition depends on the ion species which were used and its energies [25,26].

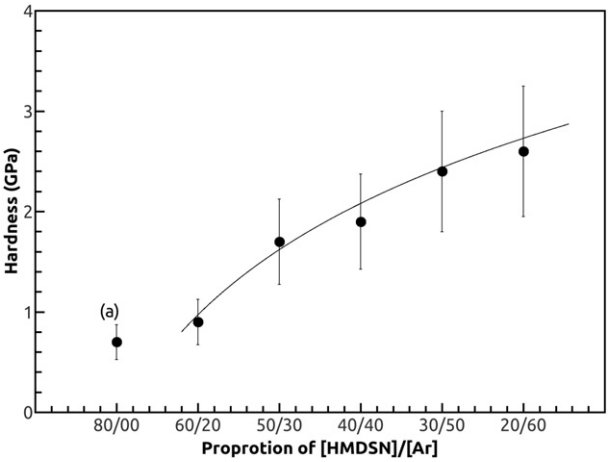

Fig. 4. Hardness of HMDSN(mTorr)/Ar(mTorr) PIIID films deposited at 50 W radio-frequency power. In (a) the film was deposited at 80 mTorr of HMDSN.

2.5. Wettability

Fig. 5 shows the contact angle and surface energy of the films measured right after deposition. As can be noticed, the as-deposited films are hydrophobic since its contact angle is 98°. Wettability is slightly

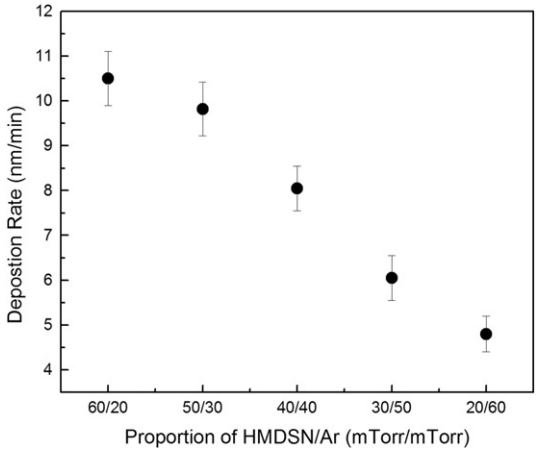

Fig. 3. Deposition rate of HMDSN(mTorr)/Ar(mTorr) PIIID films deposited at 50 W radio-frequency power.

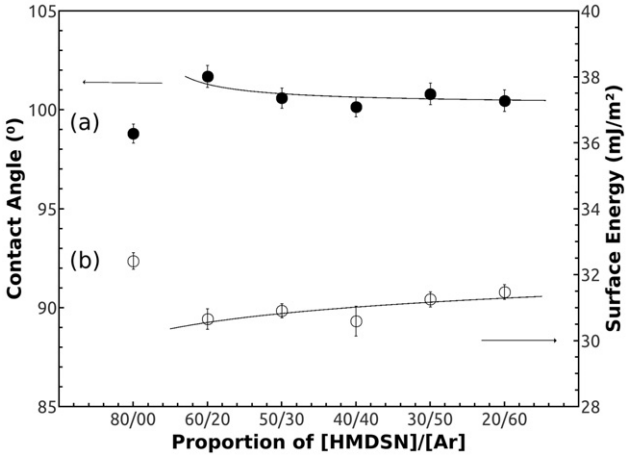

Fig. 5. Contact angle and surface energy of HMDSN(mTorr)/Ar(mTorr) PIIID films deposited at 50 W radio-frequency power. In (a) and (b) the films were deposited at 80 mTorr of HMDSN.

increased as the films are deposited in different plasma HMDSN/Ar ratio, from HMDSN(60)/Ar(20) to HMDSN(20)/Ar(60). The fall of the contact angle can be explained by the probable introduction of polar groups on the surface and structure of the samples [27]. When ions penetrate the polymer film, bond scission happens preferentially to weakly bonded species, such as hydrogen in chain terminations or lateral groups among other reactions. [28] This generates dangling bonds on the structure. Depending on the concentration and distance of the radicals, as well as of the chain mobility, such radicals do not recombine with each other and are trapped in the structure. As in contact with atmosphere, residual radicals can react with oxygen incorporating polar groups in the film structure [28]. This oxidation reaction can also occur during the deposition, if residual oxygen exists inside the reactor as it was discussed before. This interpretation is corroborated by the surface energy results, shown in the same Fig. 5. Similar results to these were observed in films produced by PIIID with HMDSN/nitrogen [3].

3. Conclusions

HMDSN/Ar PIIID films can be modified by using different argon proportions in HMDSN/Ar, whose effect is more effective when argon increases in comparison with HMDSN. The results of infrared measurements showed groups which were not present in HMDSN monomer, but were present in the films because PIIID produces films with cross-linking structure and formed by free radicals. As argon rate increases in the plasma, the films became thinner and harder, probably due to combined effect of sputtering and cross-linking. The hydrophobic character of the films was preserved regardless of the argon proportion in the plasma HMDSN/Ar mixture.

Acknowledgments

The authors would like to thank CNPq (National Counsel of Technological and Scientific Development) for the financial support.

References

[1] R.W.Y. Poon, J.P.Y. Ho, X. Liu, C.Y. Chang, P.K. Chu, K.W.K. Young, W.W. Lu, M.C. Cheung, Improvements of anti-corrosion and mechanical properties of NiTi orthopedic materials by acetylene, nitrogen and oxygen plasma immersion ion implantation, Nucl. Inst. Methods B 237 (2005) 411–416.
[2] R.K.Y. Fu, I.T.L. Cheung, F.Y. Mei, C.H. Shek, G.G. Siu, P.K. Chu, M.W. Yang, X.Y. Leng, X.X. Huang, X.B. Tiang, S.Q. Yang, Surface modification of polymeric materials by plasma immersion ion implantation, Nucl. Inst. Methods B 237 (2005) 417–421.
[3] F.V.P. Kodaira, R.P. Mota, V.A. Hills, R.Y. Honda, M.E. Kayama, K.G. Kostov, M.A. Algatti, Thin films generated by plasma immersion ion implantation and deposition of hexamethyldisilazane mixed with nitrogen in different proportions, J. Phys. Conf. Ser. 370 (2012)http://dx.doi.org/10.1088/1742–6596/370/1/012028.
[4] J. Sui, W. Cai, Mechanical properties and anti-corrosion behavior of the diamond-like carbon films, Surf. Coat. Technol. 201 (2006) 1323–1328.
[5] K.W.K. Yeung, Y.L. Chan, K.O. Lam, X.M. Liu, S.L. Wu, K.Y. Liu, C.Y. Chang, W.W. Lu, D. Chan, K.D.K. Luk, P.K. Chu, M.C. Cheung, New plasma surface treated meory alloys: towards a new generation of smart orthopedic materials, Mater. Sci. Eng. C 28 (2008) 454–459.
[6] A. Anders, Metal plasma immersion ion implantation and deposition: a review, Surf. Coat. Technol. 93 (1997) 158–167.
[7] J.Y. Chen, L.P. Wang, K.Y. Fu, N. Huang, Y. Leng, Y.X. Leng, P. Yang, J. Wang, G.J. Wan, H. Sun, X.B. Tian, P.K. Chu, Blood compatibility and sp^3/sp^2 contents of diamond-like carbon (DLC) synthesized by plasma immersion ion implantation-deposition, Surf. Coat. Technol. 156 (2002) 289–294.
[8] A. Anders, From plasma immersion ion implantation to deposition: a historical perspective on principles and trends, Surf. Coat. Technol. 156 (2002) 3–12.
[9] A. Anders, Handbook of Plasma Immersion Ion Implantation and Deposition, Wiley, London, 2000.
[10] C. Pakpum, N. Pasaja, D. Boonyawan, P. Suanpont, P. Srisantithum, C. Silawatshananai, T. Vlaithong, Diamond-like carbon formed by plasma immersion ion implantation and deposition technique on 304 stainless steel, Solid State Phenom. 107 (2005) 129–132.
[11] R.M. Oliveira, M.S. Vieira, M. Ueda, A. Toth, Growth of ZnO nanostructures on Si by means of plasma immersion ion implantation and deposition, Vacuum 89 (2013) 163–167.
[12] A.E. Kiv, E.P. Britavskaya, Diffusion processes caused by plasma immersion ion implantation, N. Technol. 5 (2001) 85–89.
[13] T. Lu, Y. Qiao, X. Liu, Surface modification of biomaterials using plasma immersion ion implantation and deposition, Interface Focus 2 (2012) 325–336.
[14] E.C. Rangel, P.A.F. Silva, R.P. Mota, W.H. Schreimer, N.C. Cruz, Thin polymer films prepared by plasma immersion ion implatation and deposition, Thin Solid Films 473 (2005) 259–266.
[15] R.M. Oliveira, M. Ueda, B. Moreno, E. Abramof, A novel process for plasma immersion ion implantation and deposition with ions from vaporization of solid targets, Phys. Status Solidi C 5 (2008) 893–896.
[16] P.K. Chu, Recent developments and applications of plasma immersion ion implatation, J. Vac. Sci. Technol. B 22 (2004) 289–296.
[17] E. Vassallo, A. Cremona, F. Ghezzi, F. Delera, L. Laguardia, G. Ambrosone, U. Coscia, Structural and optical properties of amorphus hydrogenated silicon carbonitride films produced by PECVD, Appl. Surf. Sci. 252 (2006) 7993–8000.
[18] R.Y. Honda, R.P. Mota, R.G.S. Batocki, D.C.R. Santos, T. Nicoleti, K.G. Kostov, M.E. Kayama, M.A. Algatti, N.C. Cruz, L. Ruggiero, Plasma polymerized hexamethyldisilazane treated by nitrogen plasma immersion ion implantation technique, J. Phys. Conf. Ser. 167 (2009)http://dx.doi.org/10.1088/1742=6596/167/1/012055.
[19] R. D'Agostino, D.L. Flamm, O. Auciello, Plasma Deposition, Treatment, and Etching of Polymers, Academic Press, San Diego, 1990http://dx.doi.org/10.1016/B978-0-12-200430-8.50003-8.
[20] D.C.R. Santos, R.P. Mota, R.Y. Honda, N.C. Cruz, E.C. Rangel, Plasma-polymerized acetylene nanofilms modified by nitrogen ion implantation, Appl. Surf. Sci. 257 (2013) 88–93.
[21] J.I. Cisneros, G.B. Rego, M. Tomyiama, S. Bilac, J.M. Gonçalves, A.E. Rodrigues, Z.P. Arquello, A method for the determination of the complex refractive index of non-metalic thin films using photometric measurements at normal incidence, Thin Solid Films 100 (1983) 155–167.
[22] R.P. Mota, D. Galvão, S.F. Durrant, M.A.B. Moraes, S.O. Santos, M. Cantão, HMDSO plasma polymerization and thin film optical properties, Thin Solid Films 270 (1995) 109–113.
[23] E.C. Rangel, N.C. Cruz, D.C.R. Santos, M.A. Algatti, R.P. Mota, R.Y. Honda, P.A.F. Silva, M.S. Costa, M.H. Tabacniks, Argon ion implatation inducing modifications in the properties of benzene plasma polymers, Nucl. Inst. Methods Phys. Res. B 191 (2002) 700–703.
[24] I. Tajima, M. Yamamoto, Spectroscopic study on chemical structure of plasma polimerized hexamethyldisiloxane, J. Polym. Sci., Polym. Chem. 23 (1985) 615–622.
[25] X.B. Tian, K.Y. Fu, P.K. Chu, S.Q. Yang, Plasma immersion ion implantation of insulating materials, Surf. Coat. Technol. 196 (2005) 162–166.
[26] H. Biederman, Y. Osada, Plasma Polymerization Processes, Elsevier, London, 1992.
[27] A. Kondyurin, B.K. Gan, M.M.M. Bilek, K. Mizuno, D.R. Mckenzie, Etching and structural changes of polystyrene films during plasma immersion ion implantation, Nucl. Inst. Methods Phys. Res. B 251 (2006) 413–416.
[28] E.C. Rangel, N.M. Santos, J.R.R. Bortoleto, S.F. Durrant, W.H. Schreiner, R.Y. Honda, R.C.C. Rangel, N.C. Cruz, Treatment of PVC using an alternative low energy ion bombardment procedure, Appl. Surf. Sci. 258 (2011) 1854–1861.